

PAPER • OPEN ACCESS

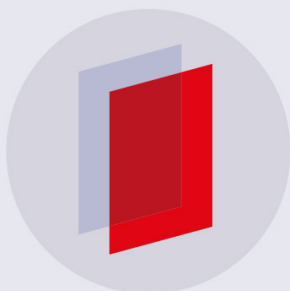
## Concept design of a disaster response unmanned aerial vehicle for India

To cite this article: Y Vashi *et al* 2017 *IOP Conf. Ser.: Mater. Sci. Eng.* **270** 012018

View the [article online](#) for updates and enhancements.

### Related content

- [Volumetric calculation using low cost unmanned aerial vehicle \(UAV\) approach](#)  
A A Ab Rahman, K N Abdul Maulud, F A Mohd *et al.*
- [Experimental result analysis for scaled model of UiTM tailless blended wing-body \(BWB\) Baseline 7 unmanned aerial vehicle \(UAV\)](#)  
R E M Nasir, A M Ahmad, Z A A Latif *et al.*
- [Land cover change mapping using high resolution satellites and unmanned aerial vehicle](#)  
N F H Jumaat, Baharin Ahmad and Hafsat Saleh Dutsenwai



**IOP | ebooks™**

Bringing you innovative digital publishing with leading voices to create your essential collection of books in STEM research.

Start exploring the collection - download the first chapter of every title for free.

# Concept design of a disaster response unmanned aerial vehicle for India

**Y Vashi, U Jai, R Atluri, M Sunjii, Y Kashyap, V Ashok, S Khilari, K Jain and S Aravind Raj\***

School of Mechanical Engineering, VIT University, Vellore – 632 014, Tamil Nadu, India

\*aravindsakthivel@hotmail.com

**Abstract.** The Indian sub-continent experiences frequent flooding, earthquakes and landslides. During the times of peril, live surveillance of the disaster zone facilitates the disaster agencies in locating and aiding the affected people. For this reason, development of a micro unmanned aerial vehicle (UAV) can be an optimal solution. This article provides a conceptualization of a UAV model that meets the need of the country. A comparison of different aircraft components and their optimization and sensitivity analyses are presented. In the end, this research produces a preliminary design of UAV that can accomplish surveillance and payload dropping missions in disaster affected areas.

## 1. Introduction

New breakthroughs in the tele-networking and signalling technologies have propelled the research and development of unmanned aerial vehicles (UAVs) throughout the globe. Although previously they are specifically for military purposes, the UAVs have been accepted by many civilian agencies within the developed as well as the developing nations for various applications. From peace time surveillance to offshore oilrig patrols, these UAVs can perform many functions that have been previously done using a full size aircraft at a fraction of the operating cost. India, with the limited regional aviation facilities, has been a scene of many natural fallouts and this situation has adversely affected the economy of the involved regions. Due to climatic changes, the country has faced scores of erratic rainfalls in previous few years. The recent South Asian floods in 2017 have killed 1300 people and affected approximately 41 million people [1]. Similarly, past floods in India especially in the states of Tamil Nadu and Bihar have seen hundreds of fatalities and displacement of the entire districts in most cases. The high rate of fatalities is directly related to the delayed response by the authorities due to shortfall of rescue assets.

With no specialised UAV at their disposal, rescue authorities have to rely on the national Air Force assets for conducting search and rescue missions, which have to be relocated from the frontline bases to the affected areas. The UAVs are used as the command and control centres to direct rescue units. To mitigate the loss of human lives and damage to the property, this study aims to offer UAV prototype that can perform the surveillance and payload dropping missions while flying close to the ground. The cause of such endeavour is to reduce losses in disaster hit areas through quick and easy surveillance by a medium sized UAV that is capable of being deployed from any short strips or roads at minimal time delay. Table 1 lists the main characteristics of a surveillance UAV according to the military standard [2]. Though the requirements of battlefield do not directly correspond to that of disaster management,



the strict limitations sanctioned by the army will facilitate in streamlining the mission statement and the meticulous design and execution.

Table 1: Characteristics of surveillance UAV

• Performance of efficient surveillance	• Maintainability	• Real time operation
• Cost-effectiveness	• Day and night operations	• Multi-mission capability
• Reliability	• Operating in a wide range of weather conditions	• Minimum turnaround time
• Usefulness and operational availability	• Beyond Line-of-Sight (BLOS) operation	

## 2. UAV Conceptual Design Phase

The mission statement for this design and development study states the requirement of a medium sized UAV with short field capabilities and a loiter time of minimum 30 minutes with full electronics and payload setup. The typical aircraft design process often includes four major phases: conceptual design, preliminary design, detail design, and test and evaluation [3]. As the name implies, aircraft conceptual design phase is when the aircraft is still at its concept level. At this stage, general design requirements are entered into the process to generate a satisfactory configuration. The summary of activities within this conceptual design phase is shown in Figure 1.

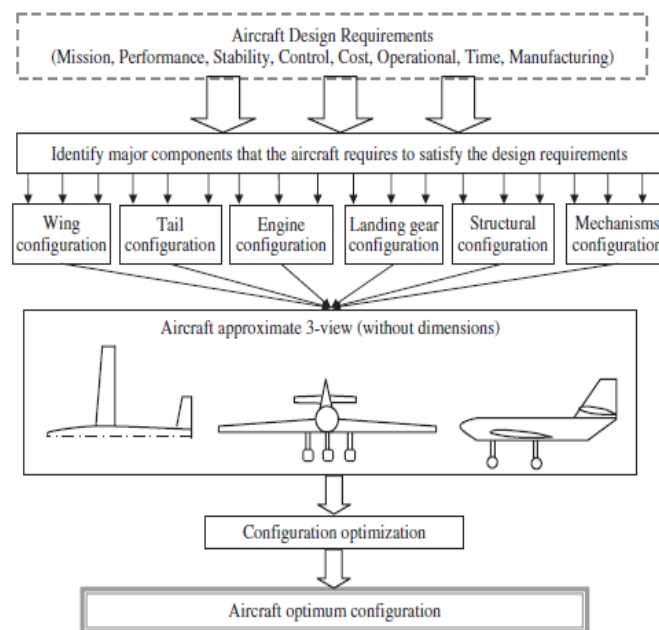


Figure 1: UAV conceptual design (reproduced from [3])

Meanwhile, Figure 2 depicts the decision making flow process that has been followed in designing the specified UAV in this study. The process involves step-by-step evaluation of the variables. During design parameter calculations such as for wing design, tail design, landing gear height, thrust required, etc., several iterations are performed with the help of C++ codes in order to eliminate the possibility of errors. The different sets of data obtained are individually evaluated with the help of aerodynamics software like XFLR, AAA and HyperWorks. Once the best set of values has been obtained, the overall aircraft parameters and planform is tested in XFLR and changes are made if necessary. Following the completion of the aircraft design concept, detailed part design of the UAV components is performed on Solid Works while the part stress analysis is performed using ANSYS. Once the required strength and

integration parameters are met, the fabrication work is performed. The fabricated UAV undergoes a thorough dimensional and structural scrutiny. Once the airworthiness of the UAV is found to comply with all safety requirements, flight tests are performed and the obtained results are compared with the calculated ones.

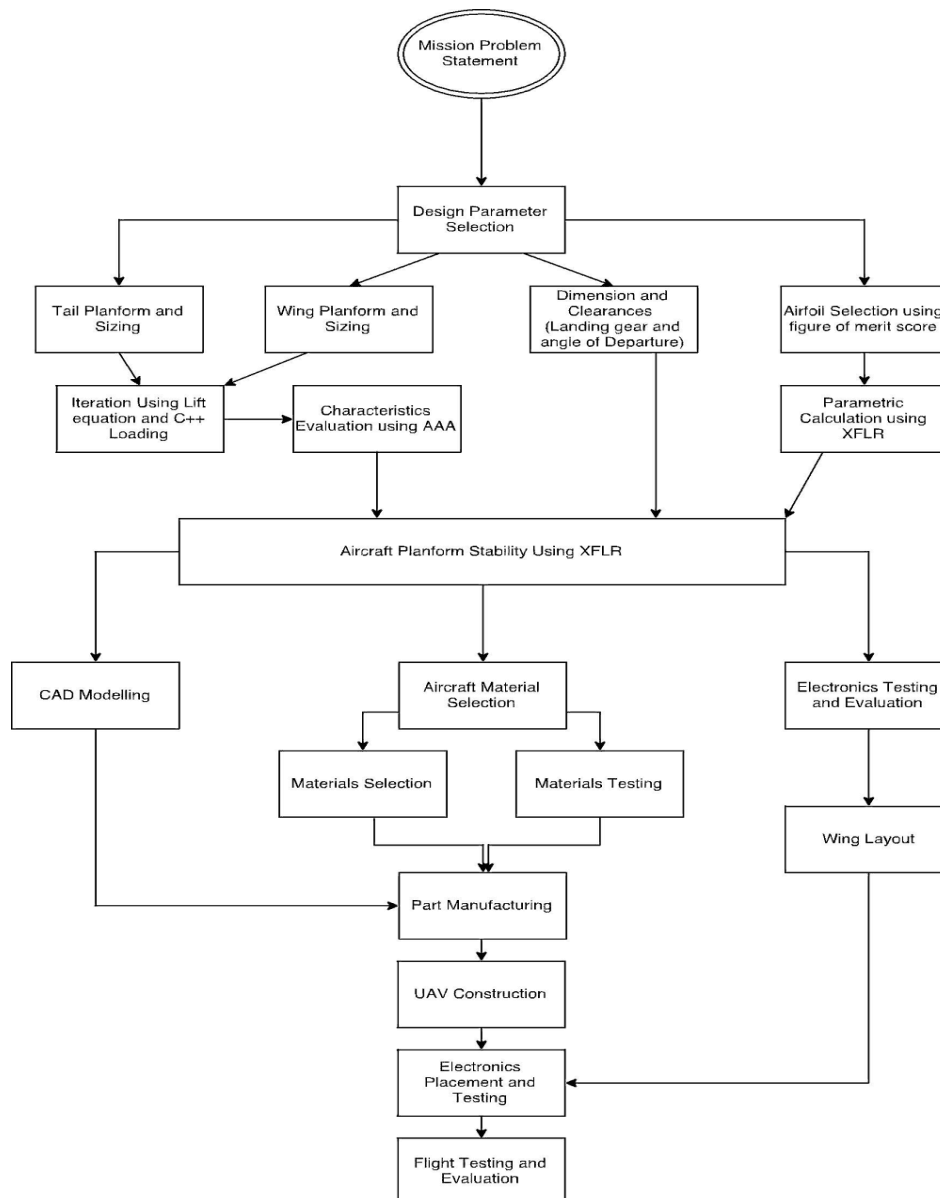


Figure 2: Methodology flowchart

The mission of the UAV is to perform surveillance and drop humanitarian packages during disaster relief. Both mission statements are represented as simple diagrams in Figure 3 and Figure 4. The static and dynamic payloads of the UAV can be varied depending on the user's requirements or the mission profile. The static payload of the UAV is generally the electronics and sensors that are carried onboard depending on the mission requirement. The sensor package may vary from a day time camera for day time surveillance to a night vision or thermal camera for night operations. The sensors may also vary from air density sensors to the sensors that can detect pollutant in the atmosphere at different altitudes. Dynamic payload of the UAV varies from medicine, food packages, location beacons for humanitarian

and rescue missions to foliage density and seismic sensors for geological missions. The calculated payload capacity of the aircraft is 24lbs, which may be optimized depending on the mission statement. For a maximum payload delivery mission, the UAV carries minimum number of batteries and more amount of dynamic payloads, whereas for a maximum endurance mission, the payload is consisted of batteries only to maximize the time on station. Therefore, the endurance of the UAV may vary from a minimum of 30 minutes to a maximum of a couple of hours depending on the setup and atmospheric conditions.

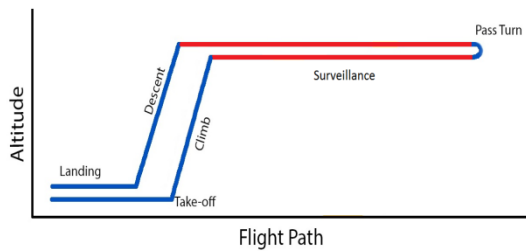


Figure 3: Flight path for surveillance mission

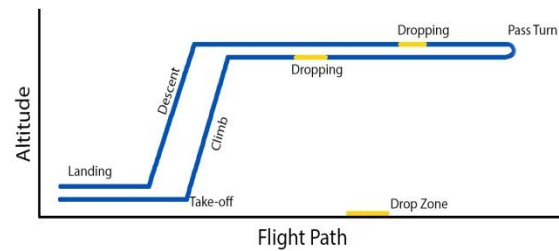


Figure 4: Flight path for dropping humanitarian aid

### 2.1. Wing Design

The wing sizing process depends on various factors including lift, drag, wing loading, span efficiency factor and others. For this study, the wing design is based on these main objectives: maximize lift to increase payload capacity, minimize drag for maximum efficiency and the UAV velocity must remain between 11-18 m/s for accurate payload dropping. Wing area, aspect ratio and the airfoil shape play a crucial role in achieving these objectives. Wing area must be maximized while the aspect ratio (AR) has to be optimized. AR determines the several parameters such as overall drag coefficient ( $C_D$ ) of the wing, overall lift coefficient ( $C_L$ ) of the wing, dimensions of the wing and hence the wing loading, and Oswald's efficiency of the wing profile ( $e$ ).

Wing sizing is done based on optimizing the variables in the lift equation. The cruise condition is used to determine the wing area and its angle of incidence. Cruising altitude of the UAV is assumed to be 200ft above the ground and the maximum speed is taken as 15m/s.  $C_L$  is 1.14 at  $7^\circ$  and using this information, cruise velocity–12m/s and wing area–1.28 m<sup>2</sup> are calculated from the Equation 1 [4].

$$L = \frac{1}{2} \rho v^2 C_L \quad (1)$$

The AR is selected as 7.33 based on the historical data of UAVs with similar mission statements [5, 6]. A higher AR will decrease drag and improve the efficiency of the wing planform but it can also compromise the structural integrity. An iterative C++ code is used to determine the optimal AR based on  $C_D$ ,  $e$  and cruise velocity at fixed lift (total payload is determined to be between 35-45 lbs), which is tabulated in Table 2. MAC is fixed at 16.5 inches. Here, the wing loading factor is not considered since the wing loading in any of the cases is very low (3-5 lbs/ft<sup>2</sup>) and does not contribute significantly to the feasibility of the design.

Table 2: Wing sizing optimization

Wing Area (m <sup>2</sup> )	AR	Velocity (m/s)	Oswald's Efficiency Factor (e)	Drag Coefficient (C <sub>D</sub> )
1.20	6.83	14.60	0.870	1.112
1.24	7.06	14.35	0.880	1.076
1.28	7.33	14.12	0.886	1.018
1.32	7.51	13.91	0.881	0.998
1.36	7.74	13.70	0.860	0.954

Based on Table 2, the optimum configuration appears to be at  $AR = 7.33$ , which corresponds to the highest  $e = 0.886$  and  $C_D = 1.018$ . The final dimensions of the wing are: wing area =  $13.78\text{ft}^2$ ,  $AR = 7.33$ , wing span = 121 inches and chord length = 1.375ft. This configuration has been tested in AVL software and the results are verified.

Wingtips are usually incorporated to change the spanwise lift distribution of the wing. In addition, it is found that wingtips also tend to reduce the induced drag produced by the wing due to the increased effective wing span that pushes the tip vortex away from the wingtip. The increase in effective wing span also means an increase in the aspect ratio of the wing, which is preferred as it offers a better lift-to-drag ratio. Often times, aspect ratio is limited by structural constraints. Therefore, wingtips provide a cost effective opportunity without necessarily straining the structural integrity of the airframe. For the proposed UAV design, winglets and Hoerner wingtips are considered. Winglets are small extensions of the wings that are usually set at an angle with respect to the surface of the wing. They can effectively reduce the magnitude of the wingtip vortices produced by the wing. However, although a well-designed winglet can reduce the induced drag, it also leads to an increase in skin friction drag at lower speeds (which covers the large proportion of the flight envelope for the UAV). This is because of its additional surface area and its form factor in general. On the other hand, Hoerner wingtips as depicted in Figure 5, do not increase the surface area significantly and therefore, do not result in the increase of skin friction drag. Moreover, the use of Hoerner wingtips result in a better span-wise lift distribution that alleviates the stress at the far ends of the wing. Based on this discussion, the Hoerner wingtips are selected and incorporated into the wings.

An important part for the wings is the airfoil shape. The airfoil selection is a crucial process, which determines the overall versatility of the UAV. Bearing in mind the subsonic flow regime around both sides of the wing and the relatively modest chord sizes, only airfoils that perform well in low Reynolds conditions are considered [8]. The data for several low Reynolds number airfoils are extracted from the open source website and compiled. By holding a minimum bar value on the lift curve slopes, the list of airfoils is sifted down to only five airfoils: CH10, S1223, FX63, GOE225 and NACA 4412 as tabulated in Table 3. The open source Vortex Lattice Code, XFLR5 [9] is applied to obtain the  $C_L$  and  $C_D$  graphs for an infinite span wing in a subsonic, incompressible flow regime. A figure of merit graph is plotted by weighing the factors of  $C_L$ ,  $C_D$  and stall characteristics as shown in Figure 6. The weighing factors is decided by considering the goals aligned with the design objectives. The 2D characteristic values of the airfoils are then input into a VLM code, Tornado to obtain the ideal  $C_L$  and  $C_D$  values for a wing with a finite span and chord. The conversion process 2D to 3D values relies on the airfoil's lift curve slope and the wing planform [10]. In this case, the latter is assumed to be rectangular to maintain the consistency of the analysis. By analyzing the results, airfoil S1223 trumps the other airfoils by providing better lift characteristics. Besides providing better lift, its stall characteristics are more favourable during flight at the edge of flight envelope.

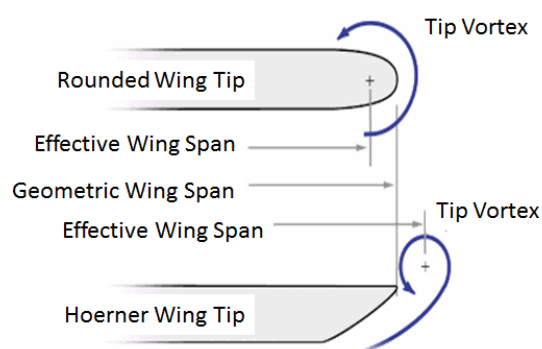


Figure 5: Hoerner wingtip [11]

Table 3: Stall angle and maximum lift coefficient for considered airfoils

Airfoil	Stall Angle (Degrees)	$C_{Lmax}$
S1223	11	2.15
CH-10	12	1.58
GOE425	10	1.36
NACA 4412	11.2	1.41
FX63-137	9	1.63

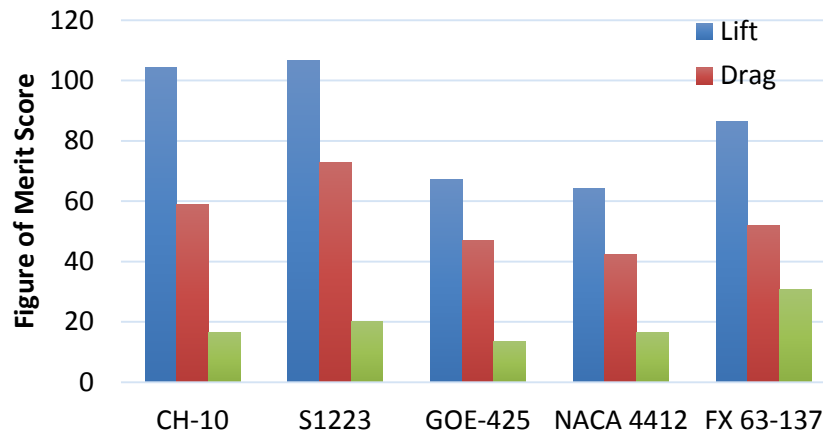


Figure 6: Airfoil comparison

### 2.2. Propulsion System Design

An aircraft requires a propulsion system to retain a sustained flight. The contribution of a power plant is to generate the propulsive force or thrust. An engine functional analysis is performed to select the right engine and determine the most suitable engine parameters. Apart from the selection, the arrangement of propulsion system also plays an important role, which can be arranged as tractor, pusher, double tractor or push-pull configuration. In the tractor type engine, engine and propeller are placed at the nose of the aircraft. It maintains the stability of the aircraft and reduces the weight of overall system. On the other hand, pusher type power plant offers safe handling characteristics, greater forward area for electronics, better field of vision for the cameras and also reduced fuselage wetted area. However, if the pusher configuration is to be used, engine cooling and propeller stall are the major factors of concern. On top of that, the pusher arrangement almost always operates in the turbulent wake of the engine and airframe that are ahead of it, which is one of the reasons its bigger noise than tractor configurations. In the push-pull type motor, propellers are placed individually on the nose and tail of the aircraft. This increases the weight of aircraft. After considering these factors, the decision of using a single tractor configuration is made.

The Jett SJ-46, a 0.46 cubic inch, two strokes, single cylinder, glow fuel engine, has been selected for the UAV. The engine is affected by the changes in climatic conditions and is tuned for the weather conditions of India [12]. Since this study is conducted in Tamil Nadu, the engine is tuned to have peak performance in regional conditions (i.e. average temperature of 32°C and humidity about 60-90% [13]. Based on the weather data obtained from Regional Meteorological Centre (RMC), Chennai, the engine is tested on multiple propellers and fuel mixtures to outperform the weather. Numerous iterations are carried out using different blends of ethanol, castor and synthetic oil blends and nitro methane [14]. A comparative study on engine temperature versus thrust generated using different fuel blends is done to understand the engine performance characteristics. For the design of the UAV, a static thrust of 7.8lbs is required for it to maintain level flight in ideal conditions and 9.86lbs of thrust in extreme weather conditions. The engine is further fine-tuned using a tuning pipe to generate additional 4lbs of thrust, considering relatively high FOS for superlative conditions. Hence, based on the mission requirements, high/low pitch propellers with different fuel blends can be used with pre-defined tuning pipe lengths to maximize the performance. An easy and user-friendly tuning-pipe length adjustment mechanism has also been made such that even a layman can operate it if required.

### 2.3. Tail Design

The overall stability of the UAV is decided by the nature of balancing forces or moments acting on it. The tail of the UAV plays a critical role in providing it with positive stability to counter and control the moment created at its wing. Adequately sized tail section provides positive handling characteristics such as pitching and yawing, and plays an important part in the recovery of the UAV. The tail design of the

UAV is based around several factors such as stability, aesthetic, structural integrity and weight. The basic function of the tail is to balance the forces, so that different tail configurations should have equal efficiency and approximately the same area. Several tail configurations like conventional tail, T-tail, H-tail and V-tail are evaluated.

Although T-tail provides the compensating phenomena and small surface sizing, the configuration requires a heavy integration for holding the configuration and the design characteristics of falling into the wing wake region at higher angle of attacks makes it unsuitable for the given task. Similarly, the H-tail provides an efficient area compensation and better stability but it proves to be a hindrance in the takeoff and landing performance of the UAV as the overhanging vertical surface reduced the departure and approach angles of the aircraft. In case of V-tail configuration, the excess weight of the integration and the surface assembly led to its rejection [4, 15]. Finally, a conventional three-piece tail design is selected. The final selected design consists of a single circular carbon fiber boom, which carries the single integration hub for both the vertical and horizon tails, thus reducing the overall tail weight of the UAV. Lightweight 6mm nylon screws and nuts are applied to fasten the structure on the circular boom, allowing for hassle free assembly and disassembly. The tail performance characteristics are quantified and compared in Figure 7, which demonstrates why conventional tail has been selected over other configurations.

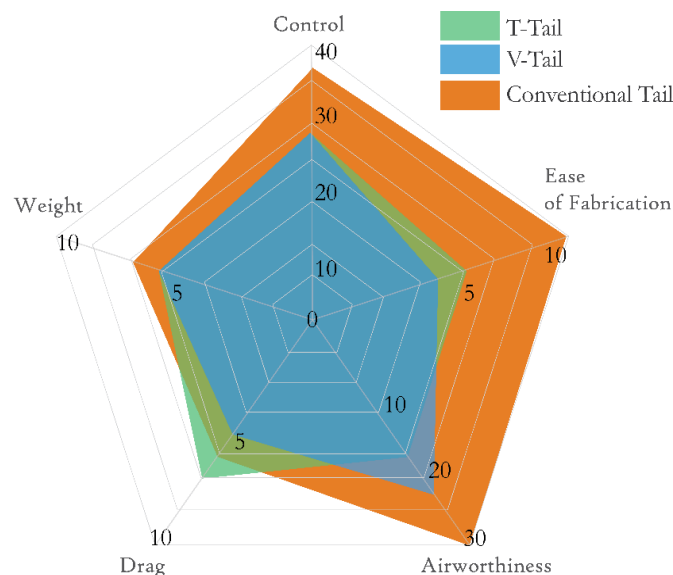


Figure 7: Tail selection

#### 2.4. Control Surfaces Design

The directional changes such as roll, pitch and yaw are brought about by the control surfaces. Accurate sizing of the control surfaces ensures safe operation of the UAV within the aerodynamic parameters such as bank angle, pitch angle, angle of attack. The ailerons located on the back of the trailing end of each wing cause movement or roll of the aircraft around its longitudinal axis. The elevator located on the horizontal tail takes care of the pitching motion on its transverse axis. Finally, the rudder mounted on rear of the vertical tail causes a movement of the UAV about its vertical axis. Each of these control surfaces is actuated by a servo motor.

From graphical data obtained from XFLR and AVL, the values for pitch, roll and yaw coefficient are found out. These data are then utilized to determine the required roll, yaw and pitch rates, and the approximate required area of the control surfaces is decided to provide the UAV with appropriate roll, pitch and yaw authority. Finally, 10% of the excess area calculated is added to compensate for the empirical or manufacturing errors.

The control surface efficiencies are evaluated using Equation 2, where  $C_l \delta_a$  is the control authority,  $y_1$ ,  $y_2$  refer the control surface distance from the root and  $C_{l_{\alpha w}}$  is the lift curve slope of the control surfaces.

$$C_l \delta_a = 2C_{l_{\alpha w}} \int_{y_1}^{y_2} cy dy \quad (2)$$

The span and cord of the ailerons are approximated at 16% and 30% of the wing of the UAV. The main factor governing the location and size of the ailerons is the desired maneuverability of the UAV. The location of ailerons also plays a major part in the structural aspect of the wing as outboard ailerons cause more twist to the wing, leading to fluttering on low aspect ratio wing. To avoid any fluttering in the wing and any potential weight increase, iterations are carried out to determine the control authority of the ailerons. Once the control authority,  $C_l \delta_a$  is determined, the dimensional value is obtained by Equation 1. The moment arm of the aileron is measured to be 5.25ft and the aileron is shown in Figure 8. In the meantime, the elevator helps with pitch and level cruise of the aircraft. A similar procedure as for the ailerons is applied to the elevator sizing process to calculate its area, chord and span required for handling the aircraft. The pitch authority of the elevator is calculated and additional dimensional margin of 5% is considered to compensate for manufacturing defects. The elevator area is set to 27% of the horizontal spanning from end to end and the elevator is shown in Figure 9. Last but not least, the main function of the rudder is to provide the UAV with yawing motion in the z-axis. The same control surface equations are used to evaluate the rudder of the vertical tail. The rudder area is calculated to be 38% of the horizontal surface area for adequate yawing of the UAV at maximum flying weight. Figure 10 illustrates the rudder designed for the UAV.



Figure 8: Aileron sizing

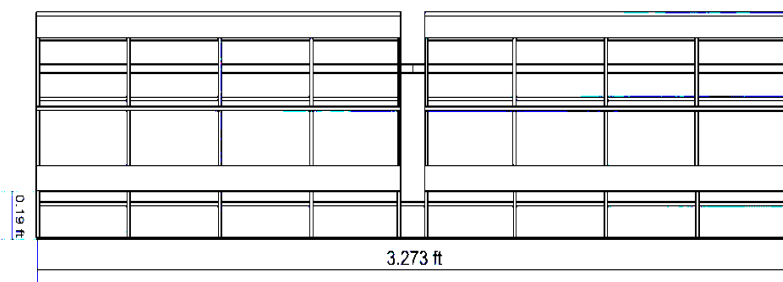


Figure 9: Elevator sizing

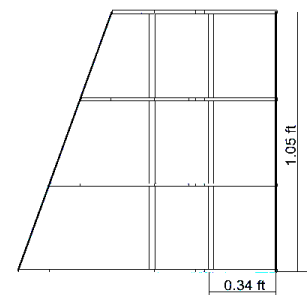


Figure 10: Rudder sizing

Selection of servos for the control surface is done by evaluating the torque required by the control surfaces using the moments acting on given surface area. Power requirements and distribution by the lithium-polymer battery is also taken into consideration. After calculating the residual power 16 kg.cm torque, turning servos are selected. To verify the authority of the aileron, a test jig simulating both the left and right ailerons is constructed. The parts simulating the ailerons are loaded with the maximum

expected load and the control surface movements are performed for a predetermined duration of flight for several cycles. Power distributions are also verified during the testing. The positioning of the servo is shown in Figure 11.

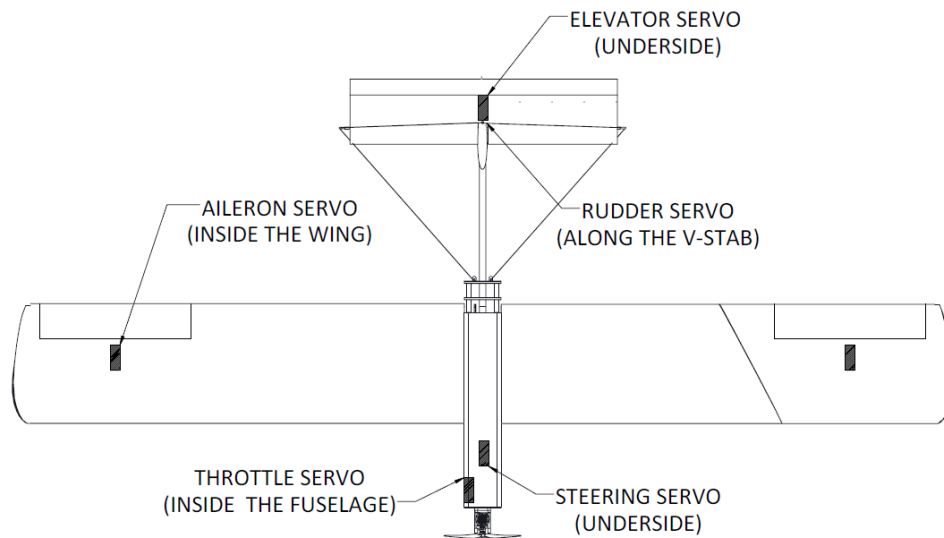


Figure 11: Servo positioning on the UAV

Stability of the UAV is of paramount importance when it comes to its maneuverability and overall endurance in rough weather conditions. Static stability is primarily influenced by tail sizing, tail arm and centre of gravity (CG) location of the aircraft. The volume coefficients are quantitative terms used to represent the effectiveness of the empennage, and they are factors at the designer's liberty and can be optimized accordingly. Volume coefficients are key values in determining the neutral point position [4]. The neutral point is always located at a distance from the CG of the UAV. This distance is termed as the static margin. It is nothing but the safe distance that the CG can shift without adversely affecting the overall the stability of the aircraft. However, having an extremely high static margin would not be feasible as it would compromise maneuverability of the vehicle. Therefore, an optimization process [16] is set up to calculate the suitable static margin that allows the control of the UAV to the pilot but at the same time will also augment the stability of the vehicle. The formula in Equation 3 gives the position of the neutral point [17], where  $x_n$  is the position of the neutral point,  $x_o$  is the position of the aerodynamic center,  $V_H$  is the volume coefficient of the horizontal stabilizer,  $a_w$  is the lift curve slope of the wing,  $a_t$  is the lift curve slope of the tail and  $\frac{\delta\varepsilon}{\delta\alpha}$  is variation of downwash with angle of attack.

$$x_n = x_o + V_H \eta \frac{a_w}{a_t} \left( 1 - \frac{\delta\varepsilon}{\delta\alpha} \right) - \frac{C_{m_{af}}}{C_{L_{aw}}} \quad (3)$$

The value of static margin is then arrived by using the position of the neutral point of 10.5% and the CG location is calculated. The stability of the UAV is then put to test in XFLR5, which has yielded the  $C_m$  vs  $\alpha$  plot. The trim angle of the aircraft (i.e. intercept of the x-axis) is established as  $0.5^\circ$ . At this angle, the UAV reaches a neutral state where all net moments acting on it would equal zero.

### 2.5. Payload Dropping Mechanism

Keeping the humanitarian nature of the UAV missions, it is provided with a dynamic payload capacity of 8lbs, which allows it to be used to drop medicines, food packs, canned containers and bottled water. In research configuration, the payload can consist of self-powered sensors to be dropped for geological readings. To keep the overall dimension and weight of the UAV to minimum, it is decided to construct an open load dropping mechanism where the dynamic payload is mounted outside the aircraft. The

dropping mechanism consists of two 16 kg-cm torque Turnigy servos that will release the drop line when triggered by the operator. To keep the drag profile of the loaded UAV low, a deflector screen is added ahead of the load and it is retracted back once the payload is released. The overall dropping is triggered with the help of the onboard camera, which relays real-time video back to the operator. The illustration of this mechanism is shown in Figure 12.

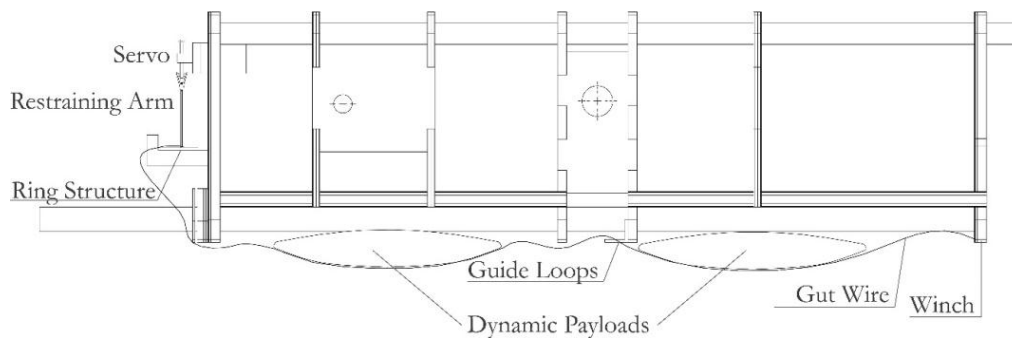


Figure 12: Payload dropping mechanism

### 2.6. Landing Gear Design

The landing gear is the principle support for the UAV when parked, taxiing, taking off and landing. It is essentially a one-dimensional structure that undergoes a large change in stress values, experiences thermal shocks and high friction, skidding and non-linear elongation from the start to end of landing or take off [18]. The landing gear configuration has several variations: bicycle, tricycle, tail dragger and multi-bogey. It can also be retractable or fixed [4]. A fixed tricycle gear is chosen as appropriate for the UAV in this study due to its supreme dynamic stability, horizontal floor angle, shorter wheel base, easiness in landing, faster acceleration during take-off due to lower angle of attack and absence of the ground looping phenomenon [3]. A fixed landing gear system increases the drag by nearly 10% but it is superior to retractable mechanism due to absence of heavy retraction mechanism. After fixing the type of gear, the overall design layout is decided by placing the main landing gear at 50-55% of the mean aerodynamic chord (MAC) of the wing. Thereafter, the distance between the aft and front CG of the UAV is calculated. The wheel base is calculated by applying 80-95% of the load on main landing gear and 5-20% on the nose landing gear [18]. The wheel track is determined such that the aircraft does not roll over when taxiing at sharp corners. The wheel and tire sizes are further calculated [4].

### 3. Conclusion

The prototype UAV is tested from both dirt and grass strips to validate the rough field short takeoff and landing characteristics. During testing, telemetric data obtained from the onboard data acquisition system has indicated a top velocity of 16m/s and a stall speed of 7m/s, which concur with calculated theoretical data. The cruise speed is obtained with a setup of static load of 16lbs and a dynamic load of 4lbs while being powered by two 5500 Mah 70C lipos. The flight endurance with the following set is obtained to be 19 minutes with the batteries being depleted to 43% charge. The designed UAV will serve the purpose of providing aerial surveillance and relief material delivery during the flood relief operations. The design parameters make it suitable for low speed cruising and also personnel detection missions. The onboard dynamic load capability allows the user to accurately deliver the relief material such as food packages or medicines and its simple and durable design will allow the relief forces to rapidly deploy this UAV from dirt strips or civil roads. The future development of the UAV will be based around a sturdier wing design to enhance its cruise characteristics by optimizing the wing aspect ratio. Lifting more dynamic cargo will be one of the key capabilities that will be maximized in order to improve mission performance of the UAV. Further enhancement will also be made on the autonomous

guidance system and onboard electronics in order to incorporate several multiple UAVs under a single command structure.

### Acknowledgement

The authors would like to thank VIT University (Vellore), School of Mechanical Engineering, Team Assailing Falcons for providing support and encouragement throughout the project. They would also like to thank Mr. Billton Vitus and Mr. Jatin Thaman for their help in the project.

### References

- [1] Dash J and Paul R 2017 <https://www.reuters.com/article/us-southasia-floods/worst-monsoon-floods-in-years-kill-more-than-1200-across-south-asia-idUSKCN1B510Z>
- [2] Schuh C A and Nieh T G 2003 *Mater. Res. Soc.* **740** 27-31
- [3] Sadrey M H 2012 *Aircraft Design: A Systems Engineering Approach* John Wiley & Sons, Ltd.
- [4] Raymer D P 2012 *Aircraft Design: A Conceptual Approach* AIAA
- [5] Tulapurkara E [http://nptel.ac.in/courses/101106035/026\\_Chapter%205%20\\_L19\\_\(03-10-2013\).pdf](http://nptel.ac.in/courses/101106035/026_Chapter%205%20_L19_(03-10-2013).pdf)
- [6] Abbott I H and Von Doenhoff A E 2012 *Theory of Wing Sections: Including a Summary of Airfoil Data* Courier Corporation
- [7] Spedding G R and McArthur J 2010 *J. Aircr.* **47** 120–8
- [8] <http://web.mit.edu/drela/Public/web/xfoil/>
- [9] Melin T 2000 *A Vortex Lattice MATLAB Implementation for Linear Aerodynamic Wing Applications* Thesis, Royal Institute of Technology (KTH)
- [10] Roskam J 2003 *Airplane Flight Dynamics and Automatic Flight Controls* Roskam Aviation and Engineering Corporation
- [11] Zenith Aircraft Company 2010 <http://www.zenithair.com/stolch801/design-wing.html>
- [12] Jett Aerotech 2015 <http://www.dubjett.com/tech2015.html>
- [13] Indian Meteorological Department 2017 [http://www.imdchennai.gov.in/obs\\_data.htm](http://www.imdchennai.gov.in/obs_data.htm)
- [14] <http://www.rccaraction.com/everything-you-need-to-know-about-nitro-fuel/>
- [15] Gudmundsson S 2014 *General Aviation Aircraft Design: Applied Methods* Elsevier
- [16] Bredehoft B, Briggs R, Chou A, Duellley R, Kovalic A, McNeilus J, Pesce P, Preus D, Prince M, Ricciardi A, Sherman M and Sunday E 2008 *Large Crowd Surveillance Unmanned Aerial Vehicle* Virginia Polytechnic Institute and State University
- [17] Anderson J D 1984 *Fundamentals of Aerodynamics* McGraw Hill
- [18] Currey N S 1988 *Aircraft Landing Gear Design : Principles and Practices* AIAA
- [19] A. Jha 2009 *14th National Conference on Machines and Mechanisms*